The bolometric output of AGN in the XMM-COSMOS survey

Elisabeta Lusso

Dipartimento di Astronomia
Università di Bologna-INAF/OABO

A. Comastri, C. Vignali, G. Zamorani, M. Brusa, E. Treister, R. Gilli, M. Bolzonella, F. Civano
and the COSMOS group.

The X-ray Universe: Berlin, June 30 2011

Prologue

Multi-wavelength database → statistically relevant sample of unobscured (Type 1, Lusso et al. 2010) and obscured (Type 2, Lusso et al., subm.) AGN.

- Broad band (from IR to X-rays) SED of Type-1/2 AGN.
- Robust estimate of the nuclear emission ($L_{\rm bol}$, $k_{\rm bol}$).
- $k_{\rm bol}$ versus $L_{\rm bol}$ at [0.5-2]keV and [2-10]keV.

Prologue

Multi-wavelength database → statistically relevant sample of unobscured (Type 1, Lusso et al. 2010) and obscured (Type 2, Lusso et al., subm.) AGN.

- Broad band (from IR to X-rays) SED of Type-1/2 AGN.
- Robust estimate of the nuclear emission ($L_{\rm bol}$, $k_{\rm bol}$).
- $k_{\rm bol}$ versus $L_{\rm bol}$ at [0.5-2]keV and [2-10]keV.

Prologue

Multi-wavelength database → statistically relevant sample of unobscured (Type 1, Lusso et al. 2010) and obscured (Type 2, Lusso et al., subm.) AGN.

- Broad band (from IR to X-rays) SED of Type-1/2 AGN.
- Robust estimate of the nuclear emission ($L_{\rm bol}$, $k_{\rm bol}$).
- $k_{\rm bol}$ versus $L_{\rm bol}$ at [0.5-2]keV and [2-10]keV.

Prologue

Multi-wavelength database → statistically relevant sample of unobscured (Type 1, Lusso et al. 2010) and obscured (Type 2, Lusso et al., subm.) AGN.

- Broad band (from IR to X-rays) SED of Type-1/2 AGN.
- Robust estimate of the nuclear emission ($L_{\rm bol}$, $k_{\rm bol}$).
- $k_{\rm bol}$ versus $L_{\rm bol}$ at [0.5-2]keV and [2-10]keV.

UV-X ray Properties

545 X-ray selected radio quiet Type 1 AGNs from the XMM-COSMOS wide field survey (2 deg^2, 1822 sources, $\langle t \rangle \sim$ 50 ks, Brusa et al. 2010)
$\longrightarrow$ **322** spectroscopically identified
$\longrightarrow$ Additional **223** AGNs with a Type 1 SED from the photo-z sample (Salvato et al. 2009)
wide range of redshift $0.04 \leq z \leq 4.25$, wide range of X-ray luminosities $40.6 \leq \log L_{[2-10]keV}\,[\mathrm{erg\,s^{-1}}] \leq 45.3$

$\alpha_{\rm ox}$ vs $L_{2500\text{Å}}$

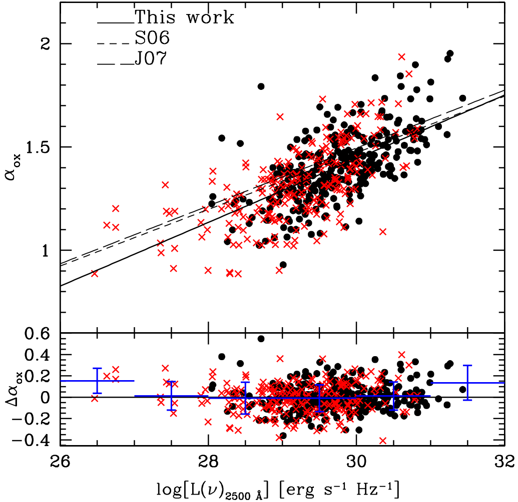

- red crosses = photometric sources
- black circles = spectroscopic sources
- slope = **0.14** for an optically selected sample (Steffen et al. 2006)
- slope = **0.15** for our X-ray selected sample
- highly significant correlation (17 σ from Kendall-τ)
- $\Delta\alpha_{\rm ox} = \alpha_{\rm ox} - \alpha_{\rm ox}(L_{2500\text{Å}})$

$\alpha_{\rm ox}$ vs $L_{2500\text{Å}}$

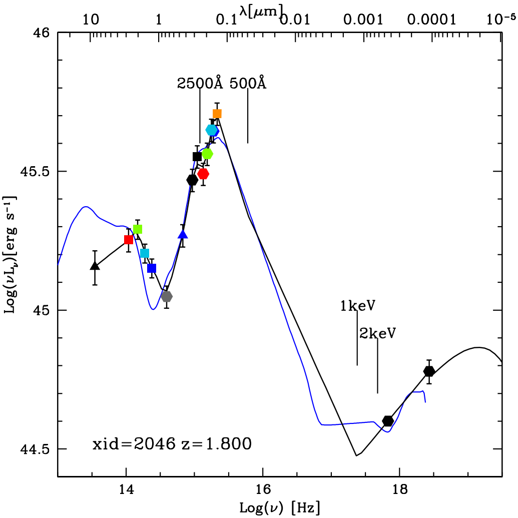

- red crosses = photometric sources
- black circles = spectroscopic sources
- slope = **0.14** for an <u>optically selected sample</u> (Steffen et al. 2006)
- slope = **0.15** for our <u>X-ray selected sample</u>
- highly significant correlation (17 σ from Kendall-τ)
- $\Delta\alpha_{\rm ox} = \alpha_{\rm ox} - \alpha_{\rm ox}(L_{2500\text{Å}})$

$\alpha_{\rm ox}$ vs $L_{2500Å}$

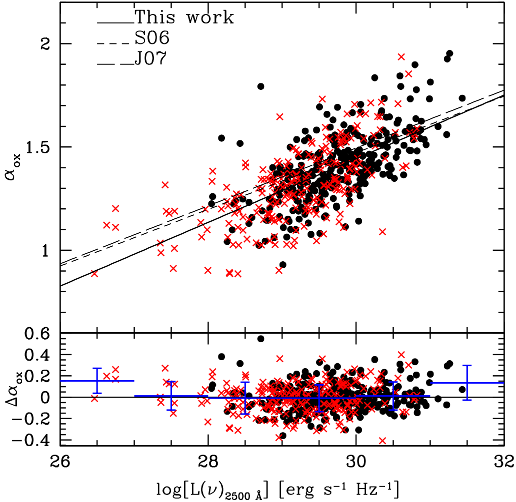

- red crosses = photometric sources
- black circles = spectroscopic sources
- slope = **0.14** for an optically selected sample (Steffen et al. 2006)
- slope = **0.15** for our X-ray selected sample
- highly significant correlation (17 σ from Kendall-τ)
- $\Delta\alpha_{\rm ox} = \alpha_{\rm ox} - \alpha_{\rm ox}(L_{2500Å})$

$k_{\rm bol}$ vs $\alpha_{\rm ox}$

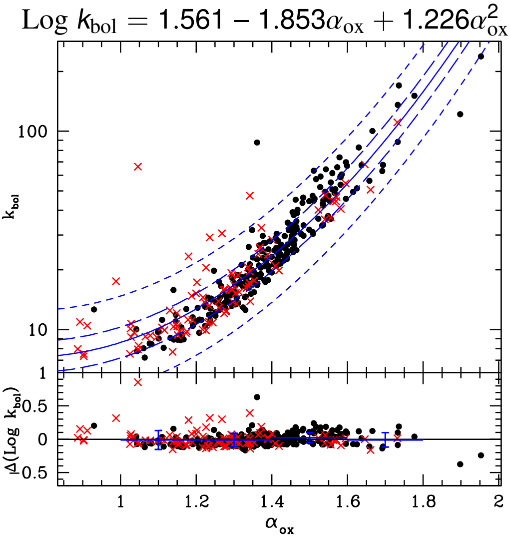

- 343 Type 1 AGN with detection in both [0.5-2]keV and [2-10]keV
- $1\ \sigma = 0.078$
  $3\ \sigma = 0.234$
- $\alpha_{\rm ox} \rightarrow$ estimate of $k_{\rm bol}$
- if the $L_{[2-10]keV}$ is available (from X-ray spectra) $\Rightarrow$ compute L_{bol}
- no need of multiwavelength data and SED extrapolation

$k_{\rm bol}$ vs $\lambda_{\rm Edd}$ and $\alpha_{\rm ox}$ vs $\lambda_{\rm Edd}$

150 Type 1 AGN with BH mass estimate (using the Mg II line width)
red open circles: 25 Type 1 AGN from Vasudevan & Fabian (2009)
high accretion rate onto SMBH → efficient accretion disk → prominent UV bump → steep $\alpha_{\rm ox}$

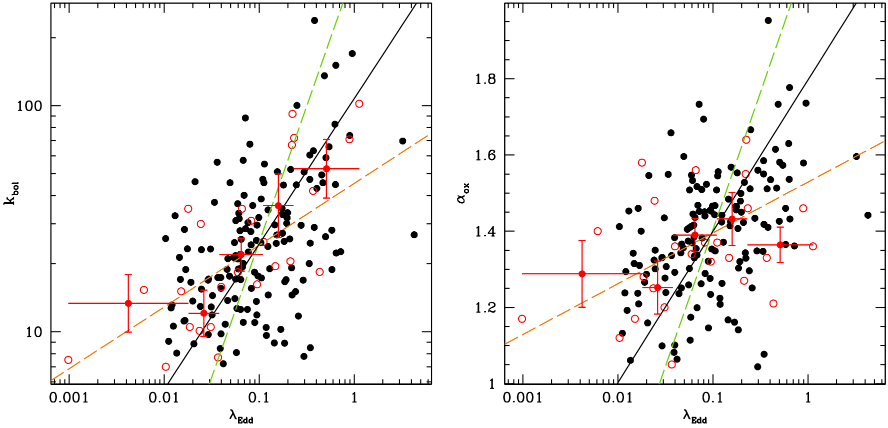

The data set

Type-2 AGN:

- **Hard X-ray sources**:
  $F_{[2-10]\mathrm{keV}} \geq 2 \times 10^{-15}$ [erg s^{-1}cm^{-2}]
  $41.06 \leqslant \mathrm{Log}\ L_{[2-10]keV} \leqslant 45.02$
- **secure** optical counterpart
- **spectroscopic** redshift $0.045 \leqslant z \leqslant 3.524$

$\Longrightarrow$ **255** Type-2 AGN

Average SED (AGN+Host-galaxy)

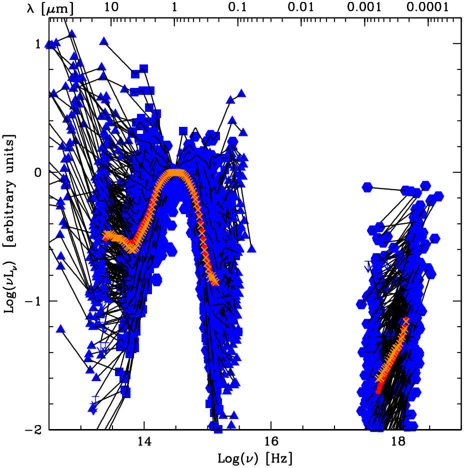

- Multi-wavelength data: SPITZER/*MIPS*: 160-70-24 μm *IRAC*: 3.6 μm-4.5 μm-5.8 μm-8.0 μm *CFHT*: J-K-i^*-u^*band *SUBARU*,*GALEX*, XMM-Newton:$[0.5-2]keV$-$[2-10]keV$.
- Rest-frame data interpolation (linear+"smoothing")
- Normalize at 1 μm luminosity
- Binning & average each bin

Average SED (AGN+Host-galaxy)

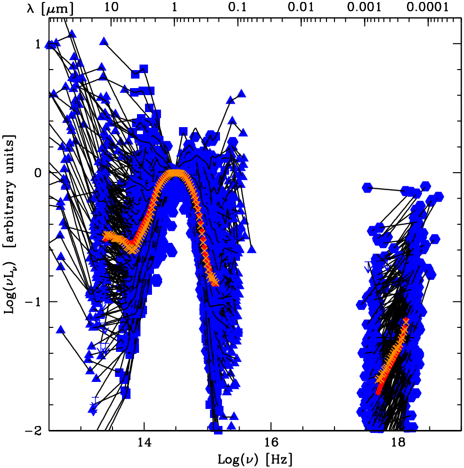

- Flat average X-ray slope $\langle \Gamma_X \rangle = 1.12$ (not corrected for $N_{\rm H}$)
- Optical-UV: dominant host-galaxy contribution
- near-IR to mid-IR: increasing contribution from the AGN,

  but very few sources with detection at 160-70 μm...
  ...waiting for far-IR data from Herschel

Binned average SED (AGN+Host-galaxy)

same number of sources in each bin: 40 AGN per bin.

z bin | IR ($8\mu m$) bin | X-ray (4 keV) bin

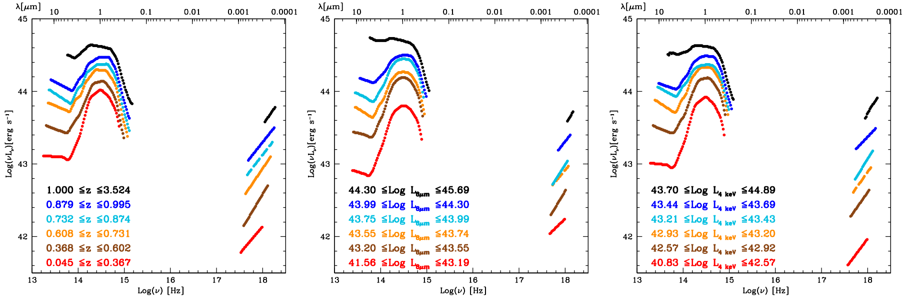

Binned average SED (AGN+Host-galaxy)

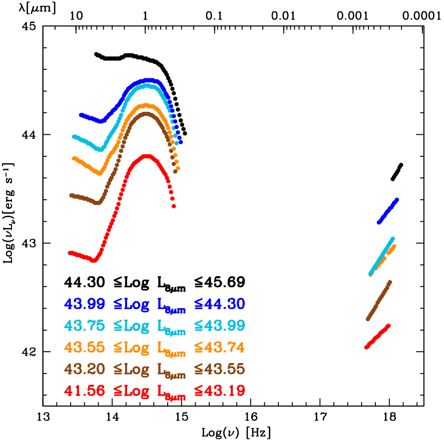

- low luminosity bins → SED "galaxy shape"
- high luminosity bins in near/mid-IR → flatter SEDs → AGN emission

SED-fitting

Main goal:
to properly disentangle the emission associated to stellar light from that due to accretion.

1. Stellar mass
2. SFR
3. AGN bolometric luminosity and bolometric correction

SED-fitting

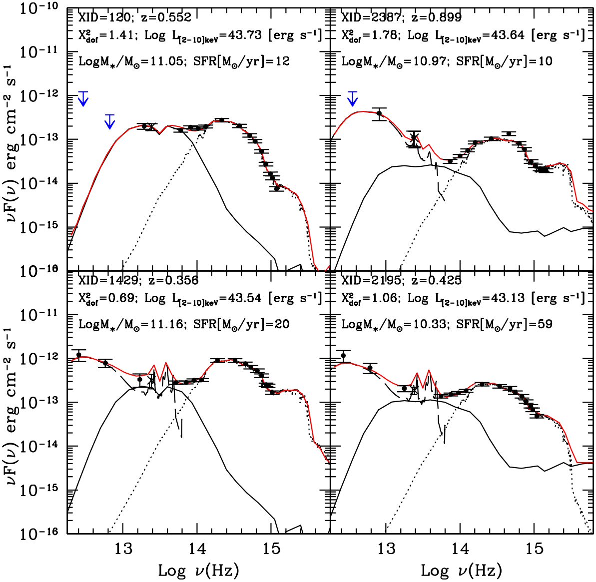

- Starburst component: Chary & Elbaz (2001), Dale & Helou (2002).
- AGN component: Silva et al. (2004)
- Galaxy component: Bruzual & Charlot (2003)

Bolometric correction

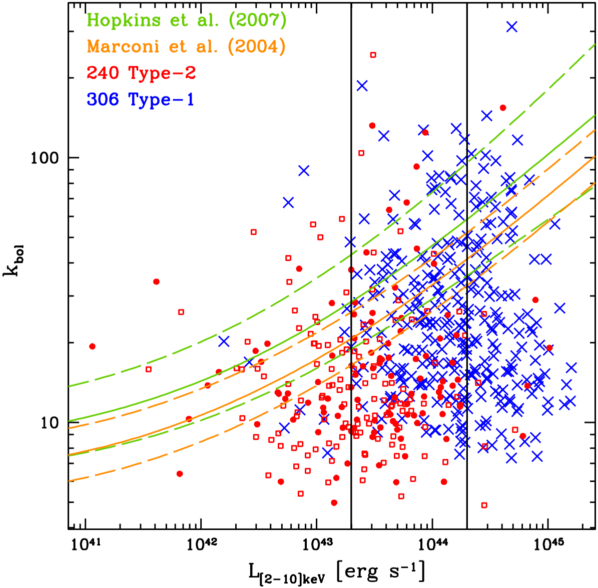

- 240 Type-2 with N_H and AGN best-fit.

  109 AGN with N_H from X-ray spectra

  131 AGN with N_H from HR.
- 306 Type-1 from Lusso et al. (2010).

Bolometric correction

AGN template spectrum from a set of power laws (enforce the relationship between the $\alpha_{\rm ox}$ and luminosity (e.g., Vignali, Brandt and Schneider 2003)→ AGN bolometric luminosity function & BH mass function

Disadvantage: no window onto the actual variation of $k_{\rm bol}$ in the real AGN population.

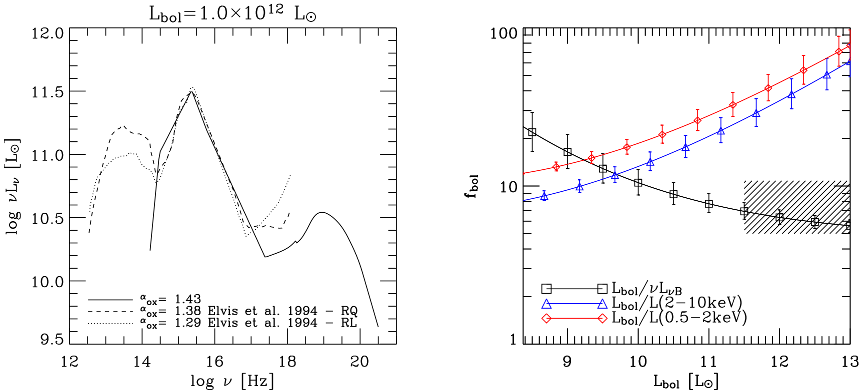

Bolometric correction

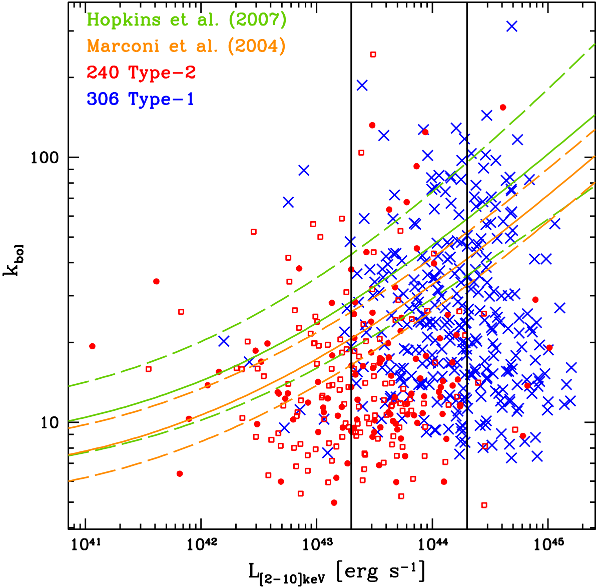

- 240 Type-2 with $N_{\rm H}$ and AGN best-fit.

  109 AGN with $N_{\rm H}$ from X-ray spectra

  131 AGN with $N_{\rm H}$ from HR.
- 306 Type-1 from Lusso et al. (2010).

$\mathrm{Log}\ L_{[2-10]\mathrm{keV}} = 43.30 \div 44.30$:

$\langle k_{\rm bol} \rangle \sim 13 \pm 1$ Type-2

$\langle k_{\rm bol} \rangle \sim 23 \pm 1$ Type-1

(significantly different at the 7σ level)

Bolometric correction

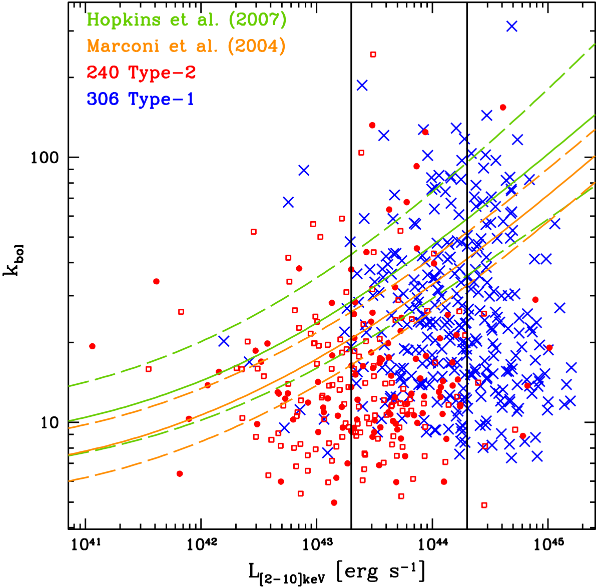

- 240 Type-2 with N_{H} and AGN best-fit.

  109 AGN with N_{H} from X-ray spectra

  131 AGN with N_{H} from HR.
- 306 Type-1 from Lusso et al. (2010).

$\mathrm{Log}\ \mathrm{L}_{[2-10]\mathrm{keV}} = 43.30 \div 44.30$:

$\langle k_{\mathrm{bol}} \rangle \sim 13 \pm 1$ Type-2

$\langle k_{\mathrm{bol}} \rangle \sim 23 \pm 1$ Type-1

(significantly different at the 7σ level)

Bolometric correction: Type-2 AGN (preliminary!!)

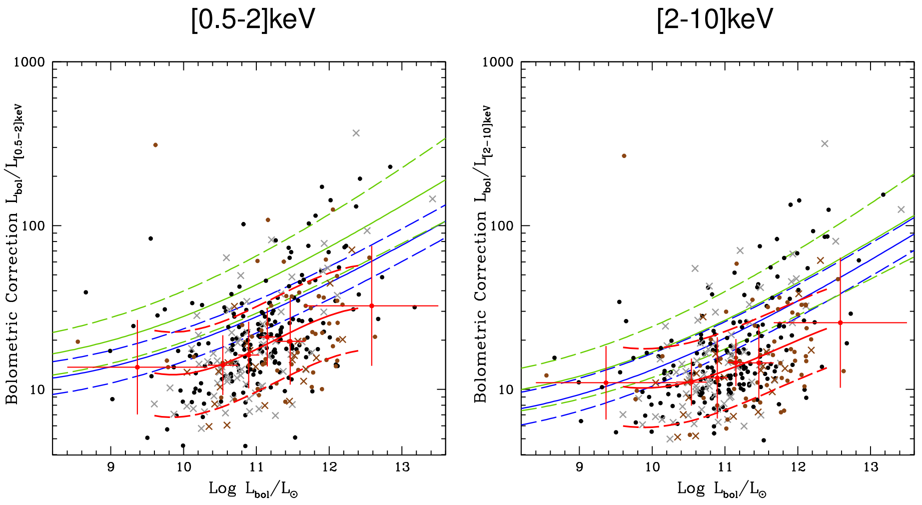

Bolometric correction: Type-1 AGN (preliminary!!)

[0.5-2]keV

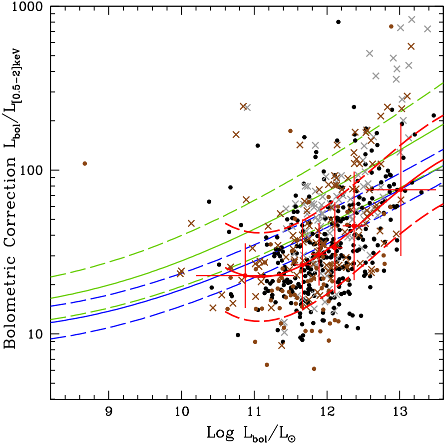

[2-10]keV

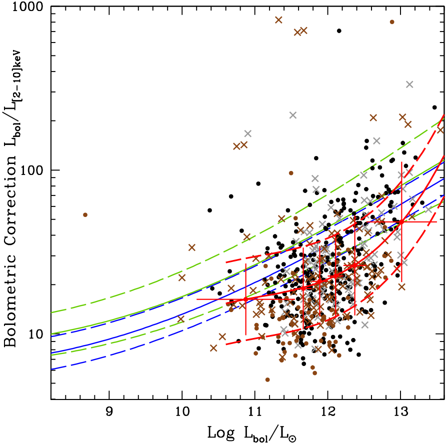

Bolometric correction: Type-1 vs. Type-2 AGN (preliminary!!)

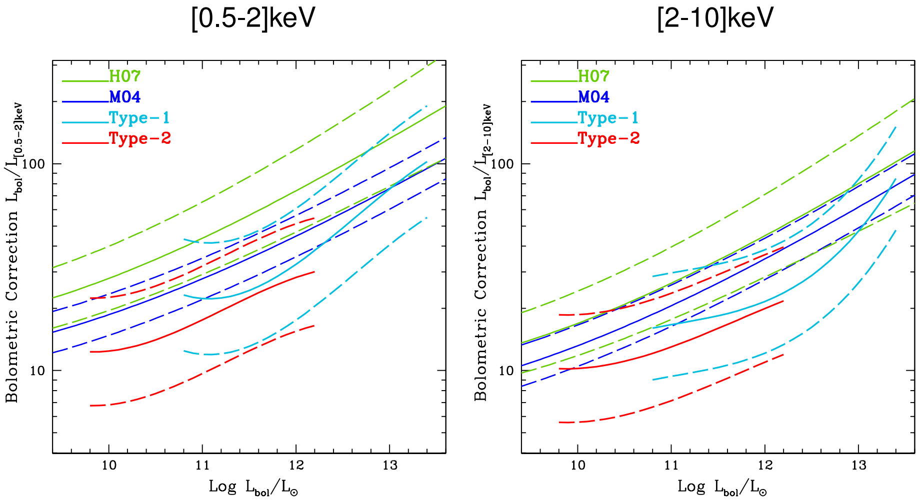

Summary & Conclusions

1. Significant correlation between α_{ox} and the UV luminosities
2. Significant correlation between both $k_{\rm bol}$ and $\alpha_{\rm ox}$ with $\lambda_{\rm Edd} = \frac{L_{\rm Bol,1\mu m}}{L_{\rm Edd}}$: high accretion rate$\Rightarrow$ large UV bump $\Rightarrow$ steep $\alpha_{\rm ox}$
3. Significant correlation between $k_{\rm bol}$ and $\alpha_{\rm ox}$: estimate of $L_{\rm bol}$ without multiwavelength data.
4. Trend of smaller $k_{\rm bol}$ for Type-2 AGN than Type-1 AGN at a given X–ray luminosity.
5. Correlation between $k_{\rm bol}$ (at [0.5-2]keV and [2-10]keV) and $L_{\rm bol}$ for both Type-1 and Type-2 AGN.